

## **The phenomenon of cavitation in grapevine... Unravelling implicated mechanisms**

### **El fenómeno de la cavitación en vid... Descifrando los mecanismos implicados**

Inés Hugalde <sup>1</sup>, Marcos Bonada <sup>2</sup>, Hernán Vila <sup>1</sup>

Originales: *Recepción:* 18/04/2017 - *Aceptación:* 07/11/2017

#### **ABSTRACT**

Cavitation is a physiological dysfunction that takes place in the xylem of water stressed plants. It leads to a loss of hydraulic conductance ( $k_L$ ) as the vessels are filled with air. This impacts water supply, water potential ( $\Psi_L$ ) and canopy hydration. Stomatal closure is an effective response upon diminishing momentary or seasonal foliar hydraulic contents. Depending on each type of plant, stomata may close preventing catastrophic cavitations. This research intended to understand how stomatal control acts upon cavitation events in two contrasting grapevine varieties, Syrah and Grenache. A mechanistic was developed model based on the water and vapour fluxes,  $k_L$ , stomata conductance ( $g_s$ ), and the vulnerability to cavitation of the xylematic tissue. The theoretical model explains how plants respond to drought and avoid catastrophic cavitation. Water stressed grapevines couple their  $g_s$  with their  $k_L$  in order to avoid embolism. It is not stomatal closure, by itself, the controlling mechanism. Grapevines under mild water stress, do not need to completely close their stomata in order to avoid cavitation, therefore, photosynthesis is not completely impeded, and the cost in terms of carbon assimilation is less than expected for other species.

#### **Keywords**

cavitation • stomatal conductance • hydraulic conductance • mechanistic model • Syrah • Grenache

---

1 INTA (Instituto Nacional de Tecnología Agropecuaria) EEA Mendoza. San Martín 3853. Luján de Cuyo, Mendoza. Argentina. [hugalde.ines@inta.gov.ar](mailto:hugalde.ines@inta.gov.ar)

2 South Australian Research and Development Institute. Waite Campus. Adelaide. SA 5064. Australia.

## RESUMEN

La cavitación es una disfunción fisiológica que ocurre en el xilema de las plantas bajo déficit hídrico, y que entraña una pérdida de su conductancia hidráulica ( $k_L$ ), cuando algunos vasos se llenan de aire. Esto incide negativamente sobre la oferta de agua y afecta el potencial hídrico foliar ( $\Psi_L$ ) y la hidratación de la canopia. El cierre estomático es una respuesta efectiva ante la disminución del contenido hídrico. Dependiendo de la especie vegetal, los estomas suelen cerrarse para evitar la cavitación catastrófica. Mediante un modelo mecanístico, que se construyó teniendo en cuenta los flujos de agua y vapor, las  $k_L$  y conductancia estomática ( $g_s$ ), y la vulnerabilidad del xilema a cavitar; se probó que  $g_s$  no es la única variable responsable de frenar la embolia. Se determinó que  $g_s$  y  $k_L$  están íntimamente asociadas y que este acople entre ambas conductancias es lo que frena la embolia. Se concluyó que, en la vid y bajo niveles de estrés hídrico moderado, no es necesario un cierre estomático para controlar la cavitación. Por esto, el mecanismo de control de la cavitación en la vid no conlleva un costo en términos de intercambio gaseoso.

### Palabras clave

cavitación • conductancia estomática • conductancia hidráulica • modelo mecanístico • Syrah • Grenache

## INTRODUCTION

Drought resistant crops have adaptive physiological and morphological traits that allow them to survive and grow under severe water deficit, resisting dehydration (14, 24). The origin of plant dehydration is embolism formation and catastrophic cavitation. In a dry soil, with low water potential, increasing xylem tension, triggers cavitation. This phenomenon consists on the formation of air bubbles inside the xylem vessels, and subsequently, the breakage of the water column (35). As consequence, the plant suffers a loss of hydraulic conductance ( $k_L$ ) and desiccation (6, 11, 34, 35). Vulnerability curves relate the percentage loss of plant  $k_L$  (PLC) or embolism to the increasing applied pressures that cause that drop of  $k_L$ . This pressure may be paralleled to the xylem tension, given that this positive pressure can be considered as equal, but opposite, to the negative pressure inside the xylem (1, 12, 31, 34).

It is well known that stomatal control prevents excessive water loss in an attempt to maintain  $k_L$  and prevent desiccation under high evaporative conditions. Several authors have also concluded that stomatal adjustment limits cavitation (4, 8, 15, 19, 21, 28) and that the mechanism is subjected to hydraulic and hydromechanic laws (3, 4, 11). In general, grapevines have been considered as drought avoiding specie due to their efficient stomatal control (8). Most of the water that enters the plant (constituting  $k_L$ ), leaves through opened stomata (depending on stomatal conductance,  $g_s$ ) as transpiration (E) (9).

In this sense, many authors have already studied the relationship between  $g_s$  and  $k_L$ , concluding that in most species, including grapevine, both conductances are tightly correlated (17, 18, 21, 29, 39). While aquaporins, in roots, act as the entrance valves for water (20, 28), stomata

in leaves act as water vapour exit valves that limit transpiration (E).

However, recent insights, cast doubt on the main role of stomatal closure on the embolism-avoidance strategy (38, 39), besides the fact that the actual involved mechanism is still not elucidated (2, 16).

In addition, grapevines have shown to own a highly resistant xylem (10) that cavitates at higher tensions than previously thought, keeping  $k_L$  between certain values before stomata respond. In this context, this research intended to study the cavitation phenomenon in grapevines and the mechanisms involved in its control. It tried to comprehend on a mechanistic manner, the stomatal functioning, its relation to the cavitation phenomenon, and the physical laws that rule them. This was achieved by complementing the construction of a functional and dynamic model with the comparison of two contrasting varieties, Syrah and Grenache, under two different water treatments, grown in pots, inside a greenhouse. These varieties were chosen because they have been reported as opposite in regards to stomatal behaviour, isohydric and anisohydric, respectively (8, 9), However, this classification is currently under strong debate (8, 14, 19, 21, 29). Given this controversy, tried to try the model as well as the varieties' behaviour under these conditions.

### Model developing

Several models have been developed describing and explaining the stomatal functioning (8). The model includes several sub-models and relates them in an attempt to explain embolism control by hydraulic traits in grapevine, adding the "vulnerability to cavitation element", and clarifying the coupling mechanism that achieves embolism control.

This model is based on the Ohm's law analogue concept (37) that states that the flow ( $J_w$ ) escaping through stomata, called transpiration (E), constitutes the impulsive force that drives water along the xylem vessels. This suction that occurs inside the xylem vessels is expressed in terms of water potential ( $\Psi$ ; MPa). Finally, this  $\Psi$  difference between soil and leaves ( $\Delta\Psi$ ) is what allows water to move from one place to the other (13, 37).

$$J_w = \frac{\Delta\Psi}{R} = k_L \cdot \Delta\Psi = E; \quad (1)$$

$$\Delta\Psi = \Psi_{soil} - \Psi_L \quad (2)$$

where:

$J_w = E$ , is transpiration ( $\text{mmol H}_2\text{O m}^{-2} \text{s}^{-1}$ )  
 $R$  = hydraulic resistance =  $1/k_H$  ( $1/(\text{mmol H}_2\text{O m}^{-2} \text{s}^{-1} \text{MPa}^{-1})$ )  
 $k_L$  = hydraulic conductance ( $\text{mmol H}_2\text{O m}^{-2} \text{s}^{-1} \text{MPa}^{-1}$ )  
 $\Delta\Psi$  = water potential difference (MPa)  
 $\Psi_{soil}$  = soil water potential (MPa)  
 $\Psi_L$  = leaf water potential (MPa)

Assuming that species like grapevines have null capacitance (25); (meaning that there is no water storage due to the water potential difference),  $J_w$  equals E (1), and may be expressed by Fick's law as follows:

$$E = \frac{(e_{sT(L)} - e_a)}{P_a \cdot (g_s^{-1} + g_b^{-1})} \quad (3)$$

where:

$E$  = transpiration ( $\text{mmol H}_2\text{O m}^{-2} \text{s}^{-1}$ )  
 $(e_{sT(L)} - e_a)/P_a = q'$  which is the difference of water vapour concentration between leaf and atmosphere, the vapour pressure gradient from leaf to air (dimensionless variable, it is a ratio of pressures).  
 $(g_s^{-1} + g_b^{-1})$  = sum of stomatal and boundary layer resistances ( $1/\text{mmol H}_2\text{O m}^{-2} \text{s}^{-1}$ ).

Then, by replacing (2) and (3) in (1), is obtained (4)

$$\Psi_L = \Psi_{soil} - \frac{q' / g_s^{-1} + g_s^{-1}}{k_L} \quad (4)$$

where:

$q'$  = vapour pressure gradient from leaf to air.

Eq. (4) formalizes the relationship between  $\Psi_L$ ,  $q'g_s$  and  $k_L$ .

The next step in this model development is to relate plant embolism (Emb) to the hydraulics described. Emb inversely depends on water potential ( $\Psi$ ). For more negative values of  $\Psi$ , higher percentages of Emb can be measured. In the model, Emb was interpreted by means of the mathematical adjustment of the sigmoid vulnerability curves of grapevines to a piece-wise defined function, shown as follows in figure 1.

In the first piece of the function, up to certain  $\Psi_L = \Psi_{L1}$ , Emb equals zero (5). This part of the function is called "lag" and corresponds to a range of  $\Psi_L$  values where no embolism takes place. When  $\Psi_L$  diminishes because of increasing water deficit, exceeding  $\Psi_{L1}$ , Emb linearly depends on  $\Psi_L$ , and grows until maximum Emb -i.e. 100%- is achieved for  $\Psi_L = \Psi_{L2}$  (6). On or after  $\Psi_{L2}$ , Emb equals 1 (or 100%; (7); figure 1).

$$\begin{cases} Emb = 0 & ; \Psi_L \leq \Psi_{L1} \end{cases} \quad (5)$$

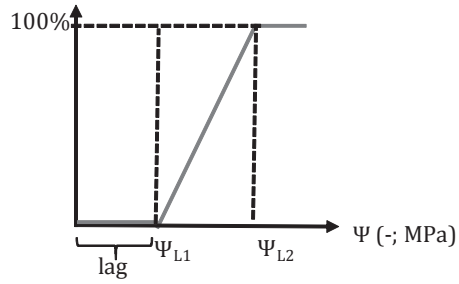
$$\begin{cases} Emb = a + b \cdot \Psi_L; \Psi_{L1} \geq \Psi_L \geq \Psi_{L2} \end{cases} \quad (6)$$

$$\begin{cases} Emb = 1 & ; \Psi_L \leq \Psi_{L2} \end{cases} \quad (7)$$

By trigonometry, equation (6) can mathematically be expressed as (8):

$$Emb = \frac{\Psi_L - \Psi_{L1}}{\Psi_{L2} - \Psi_{L1}}; \Psi_{L1} \leq \Psi_L \leq \Psi_{L2} \quad (8)$$

Then, by replacing (4) in (6) is obtained the suffered Emb as output of the model, (Equation 9), for the part of the function in which Emb linearly depends on  $\Psi_L$ .



The "lag" indicates the pressures under  $\Psi_{L1}$  where no embolism takes place. Note that  $\Psi$  are negative values.

El "lag" indica la presión bajo la cual no existe embolia. Los valores de  $\Psi$  son negativos.

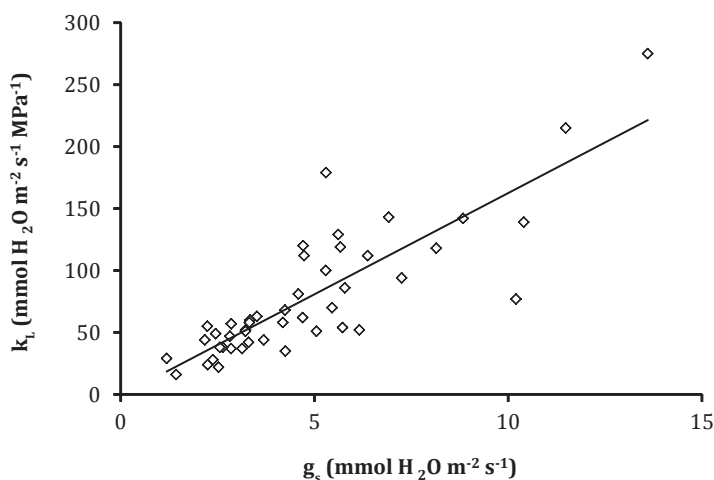
**Figure 1:** Theoretical vulnerability curve for grapevines.  $\Psi_{L1}$ , the pressure at which embolism starts, and  $\Psi_{L2}$ , the pressure at which embolism reaches its maximum value.

**Figura 1:** Curva teórica de vulnerabilidad para vid.  $\Psi_{L1}$ , la presión a la cual comienza la embolia, y  $\Psi_{L2}$ , la presión a la cual existe embolia máxima.

$$Emb = \frac{(\Psi_{soil} - \frac{q' / g_s^{-1} + g_b^{-1}}{k_L}) - \Psi_{L1}}{\Psi_{L2} - \Psi_{L1}} \quad (9)$$

Equation 9 probes that plant embolism effectively depends on  $g_s$ , although not in a direct manner, but through its interaction with other variables, like  $q'$  (that depends on leaf temperature  $T_L$  and atmospheric variables), the boundary layer conductance ( $g_b$ , that varies with wind speed) and most importantly, with  $k_L$ , that depends on root aquaporin activity (36). With respect to the  $g_s$  vs.  $k_L$  relation, it has been widely proved that they are strongly correlated throughout the day; and this study corroborated this fact ( $R = 0.8438$ ,  $p = 0.000$ , figure 2, page 37).

In this study, it is created a new variable called  $\Delta g_s$  that represents the ratio between  $g_s$  and  $k_L$ .



Values are individual measurements. / Los puntos son valores individuales de medición.

**Figure 2.** Correlation between stomatal conductance ( $g_s$ ,  $\text{mmol H}_2\text{O m}^{-2} \text{s}^{-1}$ ) and hydraulic conductance ( $k_L$ ,  $\text{mmol H}_2\text{O m}^{-2} \text{s}^{-1} \text{MPa}^{-1}$ ) for Syrah.

**Figura 2.** Correlación entre conductancia estomática ( $g_s$ ,  $\text{mmol H}_2\text{O m}^{-2} \text{s}^{-1}$ ) y conductancia hidráulica ( $k_L$ ,  $\text{mmol H}_2\text{O m}^{-2} \text{s}^{-1} \text{MPa}^{-1}$ ) para Syrah.

The model also shows the feedback relationship between Emb and  $k_L$ . This feedback process states that Emb depends on  $k_L$ , while, at the same time,  $k_L$  depends on Emb, as the former diminishes when the latter rises.

Figure 3 (page 38), shows the dynamic mechanistic model that explains how the relationship between  $g_s$  and  $k_L$  controls embolism, and how embolism, in turn, modifies  $k_L$  in a feedback loop. The  $k_L$  (2) is the result of a  $k_L$  before embolism ( $k_{Lbe}$  or maximum  $k_L$ , 3), then affected by embolism (1). The  $k_{Lbe}$  is a function of the time of day and  $\Psi_{soil}$ .

The model adopted several already existing models to fit into the general model.

The  $g_s$  (5) is interpreted by the Buckley *et al.* model (2003);  $g_b$  and leaf temperature ( $T_L$ ) are expressed by the Campbell and Norman (2012) equations (4);  $\Psi_{ng}$  (osmotic water potential of the guard cell),

included in  $g_s$  (5), is empirically expressed by Taiz and Zeiger (1998) and Tardieu and Simonneau (1998). The entry variables are  $\Psi_{L1}$ ,  $\Psi_{L2}$ , time of day (hour),  $\Psi_{soil}$ ,  $T_a$ ,  $e_a/P_a$ , wind speed and solar radiation. The model output is Embolism (1).

### Model parameterizing

To parameterize the model, it was designed an experiment with Grenache and Syrah plants, under field capacity and water stress. It was measured gas exchange and  $\Psi_L$  during a complete day, from predawn to 18 h. The  $k_L$  was calculated for each moment along the day, and a time dependent equation was then fitted to the data. Vulnerability curves were constructed and embolism achieved along the day was estimated.

$$\Psi_{L1}, \Psi_{L2}, \text{time(hour)}, \Psi_{\text{soil}}, T_a, q', \text{wind, solar radiation; entry variables} \quad (1)$$

$$\begin{cases} Emb = 0 & ; \Psi_L \leq \\ Emb = a + b \cdot \Psi_L & ; \Psi_{L1} \geq \Psi_L \leq \Psi_{L2} \\ Emb = 1 & ; \Psi_L \leq \Psi_{L2} \end{cases} \quad (2)$$

$$k_L = k_{Lbc} (1 - Emb) \quad (3)$$

$$k_{Lbc} = f(\text{time}, \Psi_{\text{soil}}) \quad (4)$$

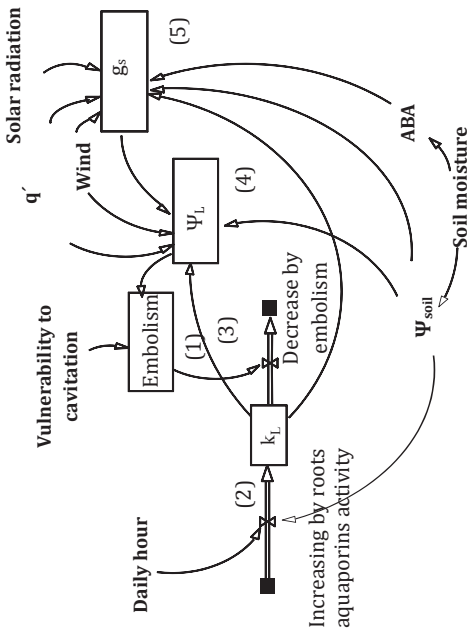
$$\Psi_L = \Psi_{\text{soil}} \frac{q' / g_s^{-1} + g_b^{-1}}{k_L} \quad (5)$$

$$g_b = 1.4 \cdot 0.147 \sqrt{\frac{\mu}{0.8} w_L}$$

$$q' = (es(TL) - ea) / Pa$$

$$\Psi_{ng} = f(\text{solar radiation}, [ABA])$$

$$g_s = \frac{x \cdot (-\Psi_{ng} + \Psi_{nc} - M \cdot \Psi_{\text{soil}} + M \Psi_{ng})}{1 - X \cdot (M \cdot k_L^{-1} - f_g \cdot r_g \cdot P)}$$



Equations on the right are represented by numbers in the figure. The ambient mechanics are formalized by the Campbell and Norman (1998) equations of boundary layer conductance ( $g_b$ ) and atmospheric deficit ( $q'$ ) that are then included in the Buckley *et al.* (2005) equation for stomatal conductance ( $g_s$ ) (5). The Van den Honert (1948) equation (4) establishes the leaf water potential ( $\Psi_L$ ) that later will define plant hydraulic conductance ( $k_L$ ). The hydraulic conductance before embolism ( $k_{Lbc}$ ) equation formalizes the relationship between maximum  $k_L$  and  $k_L$  after embolism takes place, being the formal subjected to soil water potential and daytime, according to Vandeleur *et al.* (2009). (2) and (3). Finally, the equations expressing Embolism course are shown in (1). Equation (1) defines Xylem Embolism based on the parameters that characterize the vulnerability curve of a definite species. Note that this model is constructed based on several mechanistic models, and all of them joined together in one bigger mechanistic model via the Embolism functional equation.

Las ecuaciones de la derecha se representan por números en el diagrama. Los mecanismos ambientales se formalizan mediante las ecuaciones de Campbell y Norman (1998) para la conductancia de la capa límite ( $g_b$ ) y el déficit atmosférico ( $q'$ ) que luego se incluyen en la ecuación de Buckley *et al.* (2005) para conductancia estomática ( $g_s$ ) (5). La ecuación de Van den Honert (1948) (4) define el potencial hídrico foliar ( $\Psi_L$ ) que luego definirá la conductancia hidráulica ( $k_L$ ). La ecuación de conductancia hidráulica antes de la embolia ( $k_{Lbc}$ ) formaliza la relación entre la  $k_L$  máxima y la  $k_L$  después de la embolia. La primera depende del potencial hídrico del suelo ( $\Psi_{soil}$ ) y el momento del día, según Vandeleur *et al.* (2009). (2) and (3). Finalmente, las ecuaciones que expresan el curso de la Embolia se muestran en (1). La ecuación (1) define Xylem Embolism basándose en los parámetros que caracterizan la curva de vulnerabilidad de una especie definida. Nótese que este modelo integra modelos mecanísticos previos en uno solo, mediante la ecuación de embolia de la vid.

Figure 3. The dynamic model was formulated to explain how embolism control takes place by stomatal and hydraulic coupling.

Figura 3. El modelo dinámico se construyó para explicar cómo la embolia es controlada por el acople entre la conductancia estomática e hidráulica.

## MATERIALS AND METHODS

### Vines and site

The experiment was undertaken during the season 2012/2013 at the INTA's Experimental Station, in Mendoza, Argentina.

A factorial experiment combining 2-year-old Syrah and Grenache grapevines and two water regimes was established on the summer of 2012. In quadruplicate, dormant own-rooted vines were removed from their 4-L pots and replanted on a sandy loam substrate on 15-L pots to allow good growth during the season.

Water regimes, named field capacity (FC) and water deficit (WD), were irrigated with 100% and 50% of the fraction of transpirable soil water (FTSW), respectively, as follow. Immediately after replanting all vines were irrigated to saturation and water treatments were applied; the FC treatment was watered every two days to maintain 100% FTSW whereas the WD treatment was left without irrigation for a week until it reached the targeted soil moisture of 50% FTSW (0.16 g/g). After the WD pots achieved the desired soil moisture, pots were watered every two days replenishing the transpired water. Water regimes were maintained for three months. Moisture was measured every two days using moisture probes (ECH20 EC-5 sensors, Decagon devices, USA). Vines were trained to one shoot and grown in a greenhouse with daily average temperature of 25°C and photosynthetic active radiation of 800  $\mu\text{moles m}^{-2} \cdot \text{s}^{-1}$ .

### Water potential and gas exchange measurements

A portable photosynthesis system (CIRAS-2, PP Systems, Hertfordshire U.K) was used to measure instantaneous leaf gas exchange. Measurements were carried out every two hours from 6am and 6pm.

The  $\text{CO}_2$  concentration of the incoming air was maintained at 375  $\mu\text{mol} \cdot \text{mol}^{-1}$ . The same leaves used for gas exchange assessment were used to measure leaf water potential ( $\Psi_L$ ), with the Scholander pressure chamber (Biocontrol, Córdoba, Argentina), using the procedure of Hsiao (37). Predawn water potential ( $\Psi_{PD}$ ) was considered as a proxy to soil water potential ( $\Psi_{\text{soil}}$ ).

Water vapour concentration at leaf temperature ( $e_{sT(L)}/\text{Pa}$ ; hPa), was calculated via the equation of Teten.

$$e_{sT(L)} = 6.11 \times \text{Exp} \left( \frac{17.502 \times T_L}{T_L + 240.97} \right) \quad (10)$$

where:

$T_L$  = leaf temperature

*Hydraulic conductance* was calculated through the Van den Honert law, with  $\Psi_{\text{soil}}$ ,  $\Psi_L$ , and E for every assessed moment of the day.

Leaf embolism along the day (Emb) was estimated from the daily course curves of  $\Psi_L$  and the vulnerability curves, for each plant. Both curves were related and the positive pressures achieved for the vulnerability curves were directly linked to the  $\Psi_L$  measured along the day, assigning an embolism value to each moment and plant.

### Vulnerability curves

The loss of  $k_H$  to increasing  $\Psi_L$ , i.e. cavitation, was studied by constructing vulnerability curves for each plant: after all water potential and gas exchange measurements finished, shoots were harvested and transported to the laboratory for vulnerability curves construction. Previously, every leaf was removed from the stem, and the cut surfaces were sealed with contact glue. Vulnerability



curves were constructed following the "Air Injection Long" method already described (10), using a double ended pressure sleeve connected to a Scholander pressure chamber (Biocontrol, Córdoba, Argentina;). First, the shoots were flushed for 30 minutes using distilled, degassed 5% potassium hypochlorite (KClO) solution, removing all embolisms and obtaining maximum  $k_H$  ( $k_{H_{max}}$ ). Then, successive pressure cycles were imposed. The air pressure in the chamber was increased to a specific value and held for 10 minutes before it was reduced back to zero. Air pressure was successively increased to higher levels and hydraulic measures were taken, obtaining the  $k_H$  for each cycle. Percentage loss of conductivity (PLC) was calculated for each cycle relative to  $k_{H_{max}}$ .

$$PLC = 100 \times (1 - (k_i / k_{max})) = (k_{max} - k_i) / k_{max}$$

### Statistics and data analysis

Differences between treatments were assessed by multifactor and one-way ANOVA, followed by LSD test ( $p < 0.05$ ) using Stat Graphics Plus (Statistical Graphics Corp.; StatSoft, Inc., 2003). When homogeneity of variance was not reached, non-parametrical analyses were carried out.

## RESULTS

### Water relations: water potential and stomatal conductance

The imposed water deficit had an evident effect on  $\Psi_L$ . The water deficit (WD) treatments provoked a significantly lower (more negative)  $\Psi_L$  than those of the field capacity (FC) plants. For midday water potential ( $\Psi_{md}$ ), interaction between treatments was significant (varieties vs. water treatments;  $p = 0.0333$ ). As for stomatal conductance ( $g_s$ ), the WD treatments had significantly lower values than the FC ones, for the whole day course ( $p = 0,01$ ; figure 4, page 41).

Once all vulnerability curves were obtained, each one was adjusted to a piecewise defined function as described in the "Model developing" section: The first piece of the function, where no cavitation or embolism (Emb) has already happened, is called "lag" and equals zero for Emb; while the second part of the function, showing increasing cavitation, is fitted to a straight line equation (figure 1, page 36 and figure 5, page 41).

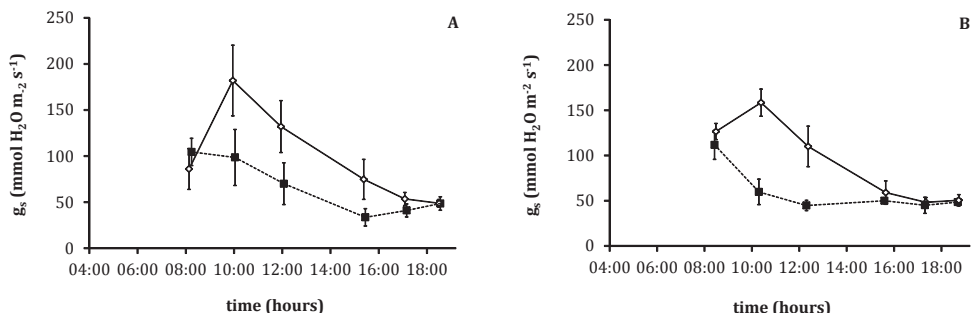
The ANOVA analysis for the straight line fitting parameters  $a$  (intercept) and  $b$  (slope) showed that neither statistically significant interaction, nor significant differences existed among varieties or water treatments (table 1, page 42). This means that under the experimental conditions, no xylem adaptation upon water stress occurred.

### Xylem embolism vs. water relations, throughout day

Estimated embolism throughout the day was only achieved in four cases, because most of the plants had vulnerability curves with long lags that started from -1.5 MPa, while this  $\Psi_L$  value was generally not achieved in the greenhouse. As leaf embolism directly depends on  $\Psi_L$ , both variables followed similar, though opposite daily courses. Lower  $\Psi_L$  corresponded to higher cavitation values (figure 6, page 42).

When it was observed the daily courses of embolism and  $g_s$  for the four plants that did cavitate, it was observed that there was no relation between both variables that could explain embolism control. Stomatal closure events (reduction on  $g_s$ ) vs. embolism detention did not correlate throughout the day, meaning that stomatal conductance, *per se*, is independent of embolism (figure 7 page 42). This conclusion was already achieved theoretically by means of the model that clearly showed that the coupling between  $g_s$  and  $k_L$  (and not  $g_s$  alone), is, in fact, the controlling switch.



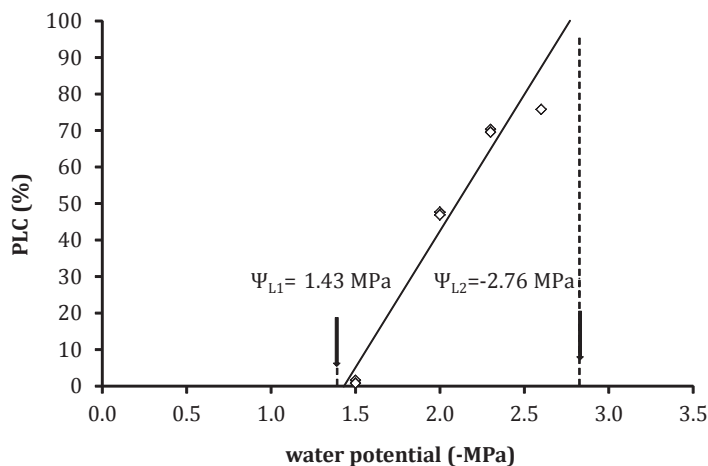


Each point corresponds to the mean  $\pm$  one SE for water deficit (WD; dotted line) and field capacity (FC; solid line) treatments.

Cada punto corresponde a la media  $\pm$  un error para déficit hídrico (WD; línea de puntos) y capacidad de campo (FC; línea entera).

**Figure 4.** Daily course of stomatal conductance ( $g_s$ ,  $\text{mmol H}_2\text{O m}^{-2} \text{s}^{-1}$ ) for Grenache (A) and Syrah (B).

**Figura 4.** Dinámica de la conductancia estomática a lo largo de un día ( $g_s$ ,  $\text{mmol H}_2\text{O m}^{-2} \text{s}^{-1}$ ) para Grenache (A) y Syrah (B).



Dots indicate values from a single shoot. Straight line indicates fitted linear curve.

Los puntos indican los valores medidos en un tallo. La línea indica el ajuste lineal obtenido.

**Figure 5.** Vulnerability curve measured in Grenache under water stress [percentage loss of hydraulic conductance (PLC) vs. pressure ( $\Psi_L$ )]. The pointed  $\Psi_{L1}$  and  $\Psi_{L2}$  are the pressures at which xylem embolism starts and equals 100%, respectively. Under  $\Psi_{L1}$  no embolism takes place.

**Figura 5.** Curva de vulnerabilidad medida en Grenache bajo estrés hídrico [porcentaje de pérdida de conductancia hidráulica (PLC) vs. presión ( $\Psi_L$ )]. Los valores de  $\Psi_{L1}$  y  $\Psi_{L2}$  señalados son las presiones a las que la embolia comenzó y alcanzó el 100%, respectivamente. Debajo de  $\Psi_{L1}$  no existe embolia.

**Table 1.** Straight line fitting parameters  $b$  (slope) and  $a$  (intercept) for vulnerability curves in Grenache and Syrah cultivars, under field capacity (FC) and water deficit (WD). Data are means and  $p$ -values are from the ANOVA.

**Tabla 1.** Parámetros de ajuste lineal  $b$  (pendiente) y  $a$  (intercepto) para curvas de vulnerabilidad en Grenache y Syrah, bajo capacidad de campo (FC) y déficit hídrico (WD). Los datos son medias de mediciones y los  $p$ -values provienen del ANOVA.

Variable	$b$	$a$
Cultivar (C)		
Grenache	-0.8855	-1.9221
Syrah	-0.8678	-1.4316
$p$ value	0.9615	0.6209
Water treatment (W)		
FC	-0.6077	-1.0930
WD	-1.1457	-2.2607
$p$ value	0.1596	0.2501
$p$ value (C $\times$ W)	0.8775	0.9983

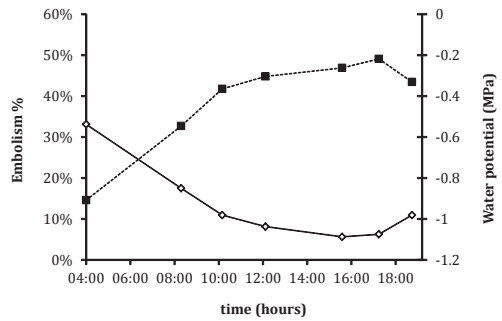


**Figure 6.** Daily course of water potential ( $\Psi_L$ ; solid line) and embolism (dotted line). Values are means from the three Syrah vines and the one Grenache plant suffering embolisms throughout the day.

**Figura 6.** Dinámica del potencial hídrico ( $\Psi_L$ ; línea entera) y la embolia (línea punteada) a lo largo del día. Los valores son la media para tres plantas de Syrah y una planta de Grenache en condiciones de embolia.

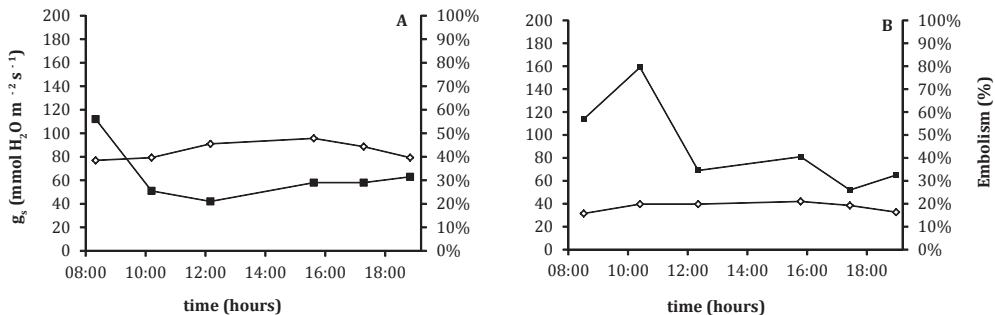


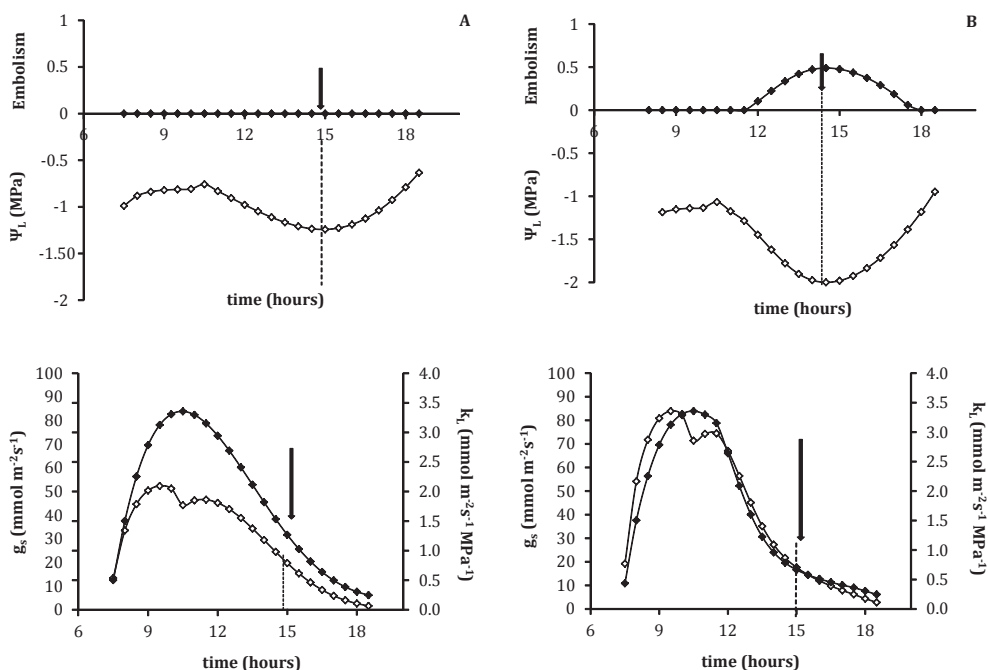
**Figure 7.** Daily course of stomatal conductance ( $g_s$ ; black squares) and embolism (black diamonds) for two vines that suffered embolism under no stress (A) and under water deficit (B). Clear independence between both curves is shown.

**Figura 7.** Cinética de la conductancia estomática ( $g_s$ ; cuadros negros) y la embolia (diamantes blancos) a lo largo de un día para dos vides que sufren embolia bajo condiciones de riego suficiente (A) y bajo estrés hídrico (B). Notar la clara independencia entre ambas curvas.

### Simulations

Figure 8, shows how embolism,  $\Psi_L$ ,  $g_s$  and  $k_L$  behaved under water stress ( $\Psi_{soil}=-0.2$ ), constant ambient circumstances and a variable guard cell osmotic adjustment ( $\pi_g$ ). The  $\pi_g$  modifies, in a significant manner, the stomatal adjustment (Buckley *et al.*, 2003). In this case, it was modified  $\pi_g$  by increasing its value by 20% for case A; and diminishing

$\pi_g$  by 20% in case B. Notice that as  $\Psi_L$  gets more negative and achieves -2 MPa, embolism starts and  $g_s$  couples with  $k_L$  ( $\Delta g_s = 28$ ), allowing a maximum embolism of 45% for simulation B. For simulation A, where  $\Psi_L$  does not grow over the threshold value and no embolism takes place, the coupling is much less evident ( $\Delta g_s = 16$ ).



Arrows in figure A show that no embolism occurs, stomatal conductance ( $g_s$ ) does not couple with hydraulic conductance ( $k_L$ ) and  $\Delta g_s=16$ . Arrows in figure B show that as soon as embolism starts, stomatal conductance ( $g_s$ ) couples with hydraulic conductance ( $k_L$ ) achieving a  $\Delta g_s=28$ . (Embolism and  $k_L$ ; black diamonds;  $\Psi_L$  and  $g_s$ ; white diamonds).

Las flechas en la figura A muestran que la embolia no ocurre, la conductancia estomática ( $g_s$ ) no se acopla con la conductancia hidráulica ( $k_L$ ) y  $\Delta g_s=16$ . Las flechas en la figura B indican que en cuanto comienza a haber embolia, la  $g_s$  se acopla con la  $k_L$  alcanzando un  $\Delta g_s=28$ . (Embola y  $k_L$ ; rombos negros;  $\Psi_L$  y  $g_s$ ; rombos blancos).

**Figure 8.** Simulations of embolism,  $\Psi_L$ ,  $g_s$  and  $k_L$  under water stress ( $\Psi_{soil}=-0.2$ ), constant ambient circumstances and variable guard cell osmotic adjustment ( $\pi_g$ ).

A:  $\pi_g$  augmented by 20%. B:  $\pi_g$  diminished by 20%.

**Figura 8.** Simulaciones de embolia,  $\Psi_L$ ,  $g_s$  y  $k_L$  bajo estrés hídrico ( $\Psi_{soil}=-0.2$ ), circunstancias ambientales constantes y ajuste osmótico de la célula guardiana variable ( $\pi_g$ ). A:  $\pi_g$  aumentado un 20%. B:  $\pi_g$  disminuido un 20%.

## DISCUSSION

These measurements and the ideated mechanistic model, demonstrated that embolism and  $g_s$  are independent. Embolism depends on  $g_s$  in addition to other physiological and ambient variables; like xylem vulnerability,  $k_L$ , difference on water vapour between leaf and atmosphere, and boundary layer conductance. In this study  $g_s$  and  $k_L$  were tightly associated ( $R = 0.70$ ). Through the model, it could be shown that the daily embolism restraint was linked to the variation that  $g_s$  suffered in intimate relation with  $k_L$ , and not to  $g_s$  itself. This tight relation between both conductances has already been widely observed in grapevine and trees (17, 21, 29, 39). This puts in evidence that  $g_s$  responds to variations in  $k_L$ ; and that both variables, in mutual interaction, control embolism in grapevines.

Apparently,  $k_L$  and  $g_s$  are related because, under drought, stomata operate allowing photosynthesis and preventing desiccation at the same time (7, 8). Consequently,  $g_s$  must respond to  $k_L$ , since changes in  $k_L$  influence plant and leaf water status (17). Therefore, the effect of  $g_s$  as prime embolism restraint attributed in grapevines and other species, could be related to the fact that both conductances are strongly coordinated (21, 29, 39).

In relation to the generated model, it should be settled that the input variable  $k_L$  is affected by the intrinsic embolism level, including a feedback process.

The model measures the phenomenon while  $k_L$  grows, (and it grows despite of the portion of hydraulic conductivity that embolism captures, probably by the action of the root aquaporins) (36).

In fact, the model functions calculating embolism in a time  $t$ , from embolism in time

$t-1$  (integrated in the input variable,  $k_L$ ). This is incorrect in negative feedback mechanisms, as embolism control shows to be (30). It might also be probable that this embolism that affects  $k_L$  is, partly, responsible for the stricter coupling of  $g_s$  and  $k_L$ . Nardini and Salleo (2000), explained that in many species embolism cannot be completely avoided and that it could constitute the signal that stomata need to start closing up. This can be reinterpreted as follows: stomata actually respond to a lower  $k_L$  caused by certain embolism formation, coupling itself to this changing  $k_L$ .

The obtained vulnerability curves were not different among treatments. Therefore, for the achieved water deficit, no xylem adaptation took place. It might be possible that differences among varieties were not evidenced because the stress levels achieved were not severe enough to generate these adaptation responses. It could also be possible that the three months period during which the plants lived was not long enough to let the xylem system anatomically adapt to the stressful situation. Besides, the possibility of discriminating vulnerability differences turns to be quite hard, given that the phenomenon shows great intrinsic variability in grapevines as in other species, (21, 22, 23, 35). For this study, variation coefficient for the "lag" value was 0.55.

Of great importance is to highlight that in grapevines, embolism control does not require complete stomatal closure, meaning that photosynthesis is not completely deprived, and the assimilation cost is not as high as expected for other species.

In this experiment, under severe water stress ( $\Psi_{\text{soil}} = -0.2$  MPa, and 50% embolism)  $g_s$  was significantly reduced but never achieved complete stomatal closure. In less stressful conditions, embolism is well controlled while stomata are maintained opened.

In 2011, Zufferey *et al.* (2011) found that stomata closed up only after 90% of embolism was achieved. This means that

the plant can keep on photosynthesizing and, at the same time, avoid catastrophic cavitation (cavitation levels at which the plant cannot recover and dyes). In this sense, it is one remarkable species that may require low amounts of water, and still produce quantity and quality of fruit, without the risk of suffering severe embolism events.

## REFERENCES

1. Alder, N.; Pockman, W.; Sperry, J. S.; Nuismer, S. 1997. Use of centrifugal force in the study of xylem cavitation. *Journal of experimental botany*. 48(3): 665-674.
2. Alsina, M. M.; Smart, D. R.; Bauerle, T.; De Herralde, F.; Biel, C.; Stockert, C.; Negron, C.; Save, R. 2011. Seasonal changes of whole root system conductance by a drought-tolerant grape root system. *Journal of experimental botany*. 62(1): 99-109.
3. Buckley, T.; Mott, K.; Farquhar, G. 2003. A hydromechanical and biochemical model of stomatal conductance. *Plant, Cell & Environment*. 26(10): 1767-1785.
4. Buckley, T. N. 2005. The control of stomata by water balance. *New Phytologist*. 168(2): 275-292.
5. Campbell, G. S.; Norman, J. M. 2012. *An introduction to environmental biophysics*: Springer Science & Business Media.
6. Chaves, M. M.; Maroco, J. P.; Pereira, J. S. 2003. Understanding plant responses to drought - From genes to the whole plant. *Functional Plant Biology*. 30(3): 239-264.
7. Chaves, M.; Oliveira, M. 2004. Mechanisms underlying plant resilience to water deficits: prospects for water-saving agriculture. *Journal of experimental botany*. 55(407): 2365-2384.
8. Chaves, M.; Zarrouk, O.; Francisco, R.; Costa, J.; Santos, T.; Regalado, A.; Rodrigues, M.; Lopes, C. 2010. Grapevine under deficit irrigation: hints from physiological and molecular data. *Annals of Botany*. 105(5): 661-676.
9. Chaves, M.; Costa, J.; Zarrouk, O.; Pinheiro, C.; Lopes, C.; Pereira, J. 2016. Controlling stomatal aperture in semi-arid regions-The dilemma of saving water or being cool? *Plant Science*. 251: 54-64.
10. Choat, B.; Drayton, W. M.; Brodersen, C.; Matthews, M. A.; Shackel, K. A.; Wada, H.; Mcelrone, A. J. 2010. Measurement of vulnerability to water stress-induced cavitation in grapevine: a comparison of four techniques applied to a long-vesselled species. *Plant, Cell & Environment*. 33(9): 1502-1512.
11. Cochard, H.; Coll, L.; Le Roux, X.; Améglio, T. 2002. Unraveling the effects of plant hydraulics on stomatal closure during water stress in walnut. *Plant physiology*. 128(1): 282-290.
12. Cochard, H.; Badel, E.; Herbette, S.; Delzon, S.; Choat, B.; Jansen, S. 2013. Methods for measuring plant vulnerability to cavitation: a critical review. *Journal of experimental botany*: p. ert193.
13. Dixon, H. H. 1914 *Transpiration and the ascent of sap in plants*: Macmillan and Company. 216 p.
14. Fernández, M. E.; Passera, C. B.; Cony, M. A. 2016. Sapling growth, water status and survival of two native shrubs from the Monte Desert, Mendoza, Argentina, under different preconditioning treatments. *Revista de la Facultad de Ciencias Agrarias. Universidad Nacional de Cuyo. Mendoza. Argentina*. 48(1): 33-47.
15. Franks, P.J.; Drake, P.L.; Froend, R. H. 2007. Anisohydric but isohydrodynamic: seasonally constant plant water potential gradient explained by a stomatal control mechanism incorporating variable plant hydraulic conductance. *Plant, Cell & Environment*. 30(1): 19-30.

16. Gerzon, E.; Biton, I.; Yaniv, Y.; Zemach, H.; Netzer, Y.; Schwartz, A.; Fait, A.; Ben-Ari, G. 2015. Grapevine anatomy as a possible determinant of isohydric or anisohydric behavior. *American journal of enology and viticulture*: p. ajev. 2015.14090.
17. Hsiao, T. C. 1990. Measurements of plant water status. In *Irrigation of agricultural crops*, B. A. Stewart and D. R. Nielsen, Editors. ASA, CSSA, SSSA: Madison. p. 243-279.
18. Hubbard, R. M.; Ryan, M.; Stiller, V.; Sperry, J. S. 2001. Stomatal conductance and photosynthesis vary linearly with plant hydraulic conductance in ponderosa pine. *Plant, Cell & Environment*. 24(1): 113-121.
19. Hugalde, I. P.; Vila, H. F. 2014. Isohydric or anisohydric behaviour in grapevine..., a never-ending controversy? *RIA (Revista de Investigaciones Agrpecuarias)*. 40(1): 75-82.
20. Javot, H.; Maurel, C. 2002. The role of aquaporins in root water uptake. *Annals of Botany*. 90(3): 301-313.
21. Keller, M. 2015. *The science of grapevines: anatomy and physiology*: Academic Press. 522 p.
22. Lovisoló, C.; Perrone, I.; Hartung, W.; Schubert, A. 2008. An abscisic acid-related reduced transpiration promotes gradual embolism repair when grapevines are rehydrated after drought. *New Phytologist*. 180(3): 642-651.
23. Lovisoló, C.; Perrone, I.; Carra, A.; Ferrandino, A.; Flexas, J.; Medrano, H.; Schubert, A. 2010. Drought-induced changes in development and function of grapevine (*Vitis* spp.) organs and in their hydraulic and non-hydraulic interactions at the whole-plant level: A physiological and molecular update. *Functional Plant Biology*. 37(2): 98-116.
24. Lucero, C. C.; Di Filippo, M.; Vila, H.; Venier, M. 2017. Comparación de las respuestas al estrés hídrico y salino de los portainjertos de vid 1103P y 101-14Mgt, injertados con Cabernet Sauvignon. *Revista de la Facultad de Ciencias Agrarias. Universidad Nacional de Cuyo. Mendoza. Argentina*. 49(1): 33-43.
25. McDowell, N.; Pockman, W. T.; Allen, C. D.; Breshears, D. D.; Cobb, N.; Kolb, T.; Plaut, J.; Sperry, J.; West, A.; Williams, D. G. 2008. Mechanisms of plant survival and mortality during drought: why do some plants survive while others succumb to drought? *New Phytologist*. 178(4): 719-739.
26. Nardini, A.; Salleo, S. 2000. Limitation of stomatal conductance by hydraulic traits: sensing or preventing xylem cavitation? *Trees-Structure and Function*. 15(1): 14-24.
27. Phillips, N.; Ryan, M.; Bond, B.; McDowell, N.; Hinckley, T.; Cermak, J. 2003. Reliance on stored water increases with tree size in three species in the Pacific Northwest. *Tree Physiology-Victoria*. 23(4): 237-246.
28. Postaire, O.; Tournaire-Roux, C.; Grondin, A.; Boursiac, Y.; Morillon, R.; Schäffner, A. R.; Maurel, C. 2010. A PIP1 aquaporin contributes to hydrostatic pressure-induced water transport in both the root and rosette of *Arabidopsis*. *Plant physiology*. 152(3): 1418-1430.
29. Pou, A.; Medrano, H.; Flexas, J.; Tyerman, S. D. 2013. A putative role for TIP and PIP aquaporins in dynamics of leaf hydraulic and stomatal conductances in grapevine under water stress and re-watering. *Plant, Cell and Environment*. 36(4): 828-843.
30. Salleo, S.; Nardini, A.; Pitt, F.; Gullo, M. A. L. 2000. Xylem cavitation and hydraulic control of stomatal conductance in laurel (*Laurus nobilis* L.). *Plant, Cell & Environment*. 23(1): 71-79.
31. Sperry, J. S.; Saliendra, N.; Pockman, W.; Cochard, H.; Cruiziat, P.; Davis, S.; Ewers, F.; Tyree, M. 1996. New evidence for large negative xylem pressures and their measurement by the pressure chamber method. *Plant, Cell & Environment*. 19(4): 427-436.
32. Taiz, L.; Zeiger, E. 1998. *Plant Physiology*, 2nd. Ed. Sinauer. Sunderland. Massachussets. Available in: <http://dx.doi.org/10.1071/PP9840361>.
33. Tardieu, F.; Simonneau, T. 1998. Variability among species of stomatal control under fluctuating soil water status and evaporative demand: Modelling isohydric and anisohydric behaviours. *Journal of Experimental Botany*. 49(SPEC. ISS.): p. 419-432.
34. Tyree, M. T.; Sperry, J. S. 1989. Vulnerability of xylem to cavitation and embolism. *Annual review of plant biology*. 40(1): 19-36.
35. Tyree, M. T.; Zimmermann, M. H. 2002. Hydraulic architecture of whole plants and plant performance, in *Xylem structure and the ascent of sap*. Springer. p. 175-214.

36. Vandeleur, R. K.; Mayo, G.; Shelden, M. C.; Gilliam, M.; Kaiser, B. N.; Tyerman, S. D. 2009. The role of plasma membrane intrinsic protein aquaporins in water transport through roots: Diurnal and drought stress responses reveal different strategies between isohydric and anisohydric cultivars of grapevine. *Plant Physiology*. 149(1): 445-460.
37. Van den Honert, T. 1948. Water transport in plants as a catenary process. *Discussions of the Faraday Society*. 3: 146-153.
38. Zufferey, V.; Cochard, H.; Ameglio, T.; Spring, J.-L.; Viret, O. 2011. Diurnal cycles of embolism formation and repair in petioles of grapevine (*Vitis vinifera* cv. Chasselas). *Journal of experimental botany*: p. err081.
39. Zufferey, V.; Smart, D. 2012. Stomatal behaviour of irrigated *Vitis vinifera* cv. Syrah following partial root removal. *Functional Plant Biology*. 39(12): 1019-1027.

#### **ACKNOWLEDGEMENTS**

This work was supported by INTA EEA Mendoza, Argentina.

We thank Dr. Mark Matthews and Dr. Andrew McElrone (UC Davis, USA) for their critical reviews of the manuscript and valuable discussions.